

# A NOVEL ELECTRON GUN WITH AN INDEPENDENTLY ADDRESSABLE CATHODE ARRAY

Kim W. Reed, Gary E. Peña, Larry X. Schneider, Joseph M. Rudys

Sandia National Laboratories, Albuquerque NM 87185

## Abstract

The design of a novel electron gun with an array of independently addressable cathode elements is presented. Issues relating to operation in a 6.5 Tesla axial magnetic field are discussed. Simulations with the TriComp [1] electromagnetic field code that were used to determine the space charge limited tube characteristic and to model focusing of the electron beam in the magnetic field are reviewed. Foil heating and stress calculations are discussed. The results of CYLTRAN [2] simulations yielding the energy spectrum of the electron beam and the current transmitted through the foil window are presented.

## I. INTRODUCTION

This application requires that a vertical sheet electron beam be swept horizontally in a 6.5 Tesla axial magnetic field. Sweeping the beam in such a strong magnetic field is not an option, so the cathode was segmented in a horizontal array of vertical thermionic emitter stripes with a slotted grid that can be sequentially turned on from one side of the array to the other, Fig. 1.

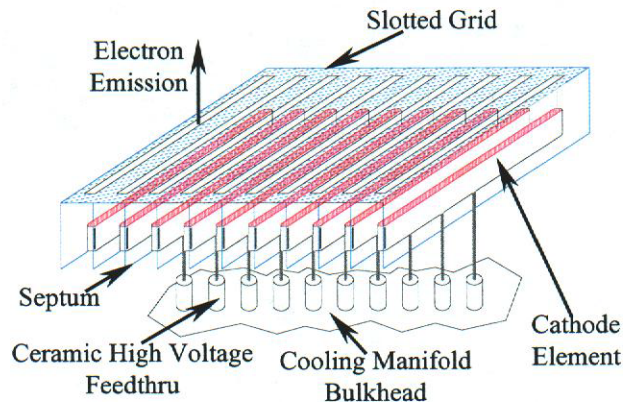


Figure 1. The cathode and grid structure.

The magnetic field is generated by a superconducting magnet with the electrical windings suspended freely in a liquid helium dewar. Since the windings are free to move in the dewar, any nearby magnetic shielding would pull the windings over to the wall of the dewar and quench the magnet. Therefore, in order to protect the electron gun control electronics from the Hall effect, they have to be

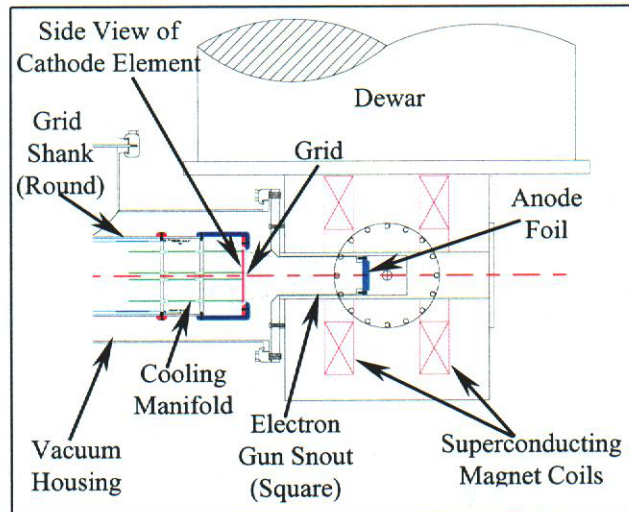


Figure 2. The electron gun and superconducting magnet.

located remotely, complicating the design. The magnet consists of a pair of toroidal windings on the same axis that produce a uniform axial magnetic field between them. A 7.62 cm x 7.62 cm square aperture opening runs through the magnet, centered on the axis of the windings. The electron gun must extend into this aperture so that the electron beam emerges from the foil window near the center of the magnet, Fig. 2. It is desired that the electron beam measure 5.08 cm x 5.08 cm at the foil window. The grid stalk is biased relative to the grounded foil window and outer vacuum housing with a DC voltage of -60 kV. If the grid shank is too close to the outer housing, in order to maximize the area of the beam, the 6.5 Tesla magnetic field will prevent the high electric fields from initiating a breakdown, but corona emission will occur. The electrons will travel down the magnetic field lines resulting in a continuous dark current on the perimeter of the foil window. In addition to causing a cooling problem at the edge of the foil, this dark current would burden the high voltage power supply and the control electronics with a continuous current drain. This problem is addressed by locating the cathode in the larger vacuum region outside the magnet and then using the converging magnetic field to focus the beam onto the foil window.

The beam emerging from the foil in the center of the magnet must have an energy distribution that peaks at 30 keV and must have an adjustable current density in the sheet beams of 0 to 5 mA/cm<sup>2</sup>. The sheet beams are



turned on by pulsing the cathode elements relative to the grid/septum structure, Fig. 1. The total duration of any given pulse is from 40  $\mu$ s to 5 ms.

## II. THE TRIODE STRUCTURE

The electron gun consists of a triode structure with a thermionic cathode that is DC biased at  $V_{cg} = 60$  kV. The rule of thumb for the maximum electrical stresses used in vacuum tubes is [3],

$$V/\text{gap} = k/(\text{gap}^{0.2}) \quad (1)$$

where,

$V$  = voltage on the gap [Volts]  
 $\text{gap}$  = electrically stressed gap [meters]

for a plane gap. For curved surfaces this electrical stress may be increased by a factor of 1.3. The value of the constant,  $k$ , is given in Table 1.

**Table 1.**  $k$  factor for electrical breakdown formula.

Pulse Length [ $\mu$ s]	$k$
1	$9.0 \times 10^6$
5	$6.0 \times 10^6$
100	$4.0 \times 10^6$
DC	$3.0 \times 10^6$

According to this formulation, the maximum allowable field over the majority of the grid shank is about 99 kV/cm. The grid shank will be made of stainless steel, having a work function by contact potential of about 4.40. If it is desired to keep the dark current to less than 0.1 mA, so that it doesn't drag down the high voltage power supply, the allowable current density based upon the 5100  $\text{cm}^2$  grid stalk area would be 20 nA/ $\text{cm}^2$ . Using the Fowler-Nordheim theory [4] and 99 kV/cm, attaining this current corresponds to being able to condition the grid shank so that the height-to-width aspect ratio of the remaining whiskers be no more than 10 to 1. This is very reasonable. If the cathode were located at the end of the snout that extends into the magnet, this condition would only allow for the beam to be 3.81 cm x 3.81 cm. Conversely, with the cathode located in the large vacuum region, outside the magnet, a TriComp analysis using the electron tracking feature, shown in Fig. 3, indicates that the beam arriving at the foil, on the right side of the figure, can be 4.57 cm x 4.57 cm. The emission surface of the cathode was chosen to be 10.16 cm x 10.16 cm and the TriComp analysis was used to determine the required axial location of the emission surface so that the outermost electrons just skim the vacuum vessel. The electrons are following the magnetic field direction from the superconducting magnet, so it is not physically possible to make the beam emerging from the foil any larger. Locating the thermionic cathode remotely

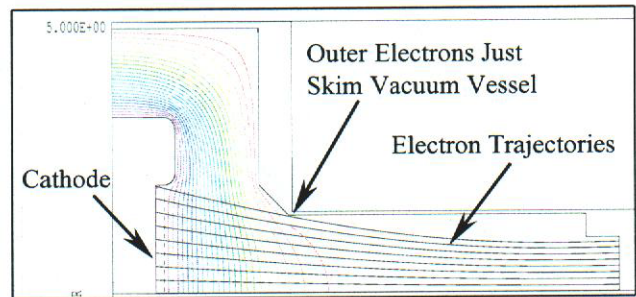


**Figure 3.** TriComp analysis showing the trajectories of the electrons emitted from the cathode.

from the foil window significantly reduces the static heat load on the foil, allowing the electron beam to be operated for longer bursts and with higher current densities.

The vacuum vessel outside the magnet is a standard 25.4 cm dia. tube, which allows the grid shank to be large while staying well below the allowable stress levels. The shank is 15.24 cm dia. The main reason, however, that this part of the vacuum vessel is so large is to maximize the pumping rate to the cathode region. Pumping rate is an issue because the BaCaO thermionic cathode must be operated at a vacuum of  $10^{-7}$  Torr or better. The matter is further complicated by the fact that all high vacuum pumps that were investigated contained some magnetic materials. In addition, cleanliness issues with the cathode rule out diffusion pumps, eddy current forces rule out turbomolecular pumps and magnetic forces on ion trajectories rule out ion pumps. It was decided to use a cryovac and locate it remotely from the magnet – this necessitates the use of high conductance lines between the pump and cathode region.

Efficiency, grid heating and foil heating issues require that attention be given to achieving maximum transmission of the electron beam through all of the structures that are in its path. To take advantage of the strong axial magnetic field a slotted grid design was selected, as shown in Fig. 1. The grid is made of 0.076 cm thick molybdenum sheet with 0.208 cm wide x 10.16 cm long slots that lie directly over and are the same dimensions as the cathode emission elements. This arrangement provides 100% electron transmission through the grid and eliminates the additional heating of the grid that would occur if it intercepted part of the beam. Molybdenum was chosen because it has a high melting point, making it compatible with the radiant heating from the thermionic cathode. An Oxide dispenser cathode can supply about 20 mA/ $\text{cm}^2$  [5], exceeding the required 5 mA/ $\text{cm}^2$  when heated to about 600°K. This puts the grid/cathode region of the triode in the space charge limited regime.

Applying the TriComp code in the space charge limited emission mode allows the current density across the grid/cathode structure as a function of voltage to be modeled, Fig. 4. Notice the increase in the current density at the inner edges of the cathodes adjacent to the center



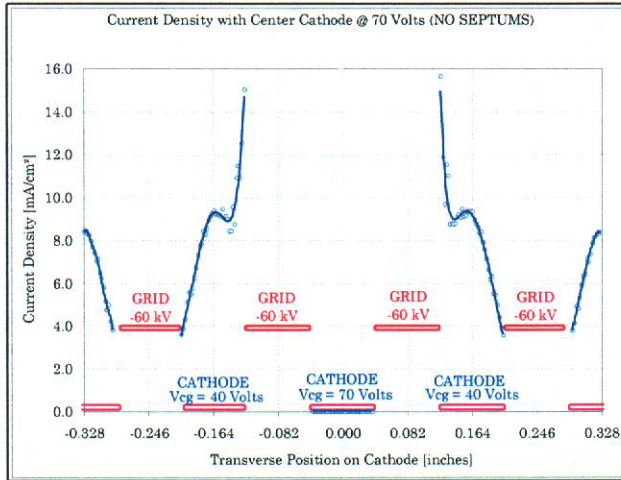


**Figure 4.** Intensification of the electrical field causes the current density to increase at the electrical potential bunching sites.

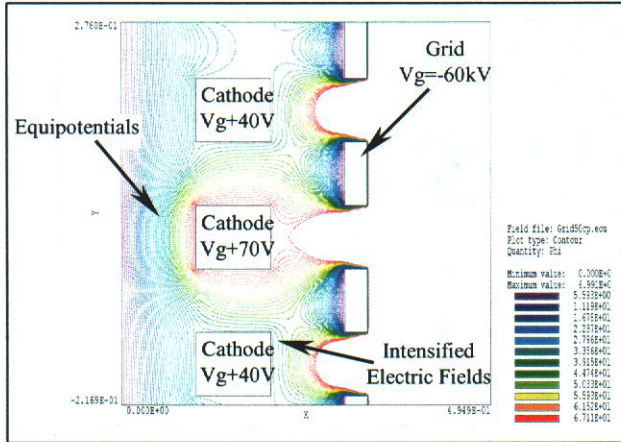


**Figure 5.** Electric fields from adjacent cathodes cause bunching of the equipotentials of nearest neighbors.

cathode that is turned off. This is caused by intensification of the electric fields at the corners of the cathodes that are adjacent to the center cathode due to its 30 Volt relative bias, Fig. 5. TriComp has served as a valuable tool, as this doubling in the current density at the edges of the two cathodes would have resulted in a broken foil window and a poisoned cathode. Further TriComp analysis shows that the cross talk between adjacent cathodes can be completely eliminated by placing a septum, at the same potential as the grid, between each of the cathodes. With the interaction between the cathode elements thus corrected, the transverse current distribution in the grid slots is roughly Gaussian.

### III. THE TUBE CHARACTERISTIC

The approximate triode tube characteristic is [6],

$$I_a = P[V_{gc} + V_{ag}/\mu]^{3/2} \quad (2)$$

where,

$I_a$  = the current leaving the cathode.

$V_{gc}$  = the voltage of the grid relative to the cathode.

$V_{ag}$  = the anode voltage relative to the grid.

$P$  = the perveance of the tube.

$\mu$  = a measure of how much the space charge limited flow in the cathode/grid region is influenced by the acceleration potential that reaches through the grid.

TriComp can be used to generate a plot of current density as a function of  $V_{gc}$  and  $V_{ac}$ . This is the tube characteristic, shown in Fig. 6.

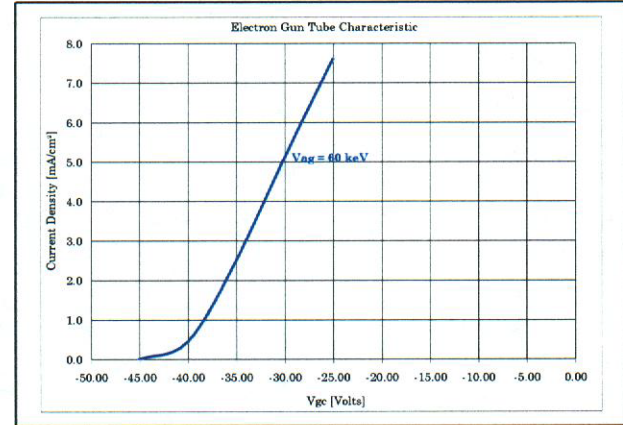


**Figure 6.** The triode tube characteristic determined from a series of TriComp runs with  $V_{ag} = 60$  kV and various values of  $V_{gc}$ .

This electron gun is designed to operate at an acceleration potential of  $V_{ag} = 60$  kV, so the tube characteristic was only calculated for that value of  $V_{ag}$ . Knowledge of the cathode voltage relative to the fixed potential of the grid that is required to turn the electron gun fully on to fully off is essential for selecting the bias power supplies and designing the control electronics. The data in Figure 6 revealed that the influence of the acceleration potential on the electrons in the region between the cathode and grid is so strong that the cathode will always be positive relative to the grid. Thus if the cathodes were biased positively relative to the high-voltage deck, then the grid could be at the potential of the high-voltage deck eliminating the need for a grid bias supply.

### IV. THE ELECTRON BEAM WINDOW

It is desired to generate an electron beam out of the beryllium foil window with a current density in the beam that is adjustable from 0 to 5 mA/cm<sup>2</sup>, an energy distribution with a peak at 30 keV and a maximum pulse duration of 5 ms. The foil has to be as flat as possible on the output side and withstand a pressure differential of 1 atm. Any one of these requirements by themselves is easy to accomplish, but a low energy beam requires a thin



foil. Foil heating due to the relatively long pulse duration and high current density reduce the yield strength of the foil. Furthermore, the foil cannot be preformed, which greatly increases the tensile stresses it will experience.

CYLTRAN was used to determine the required Be foil thickness in order to obtain the desired energy distribution out of the foil for a given input acceleration potential. It was determined that an energy distribution that peaked at the desired 30 keV, Fig. 7, could be obtained using a 60 keV acceleration potential and a 0.00254 cm thick Be foil. The analysis showed that 54% of the impinging electrons would pass through the foil. Calculations indicate that with a proper design, a hibachi with about 50% transparency to the electrons could be built. Magnetic focusing yields a current density gain of five from the cathode to the foil. Therefore only about 3.8 mA/cm<sup>2</sup> is required from the cathode to achieve the required peak current density of 5 mA/cm<sup>2</sup> at the foil.

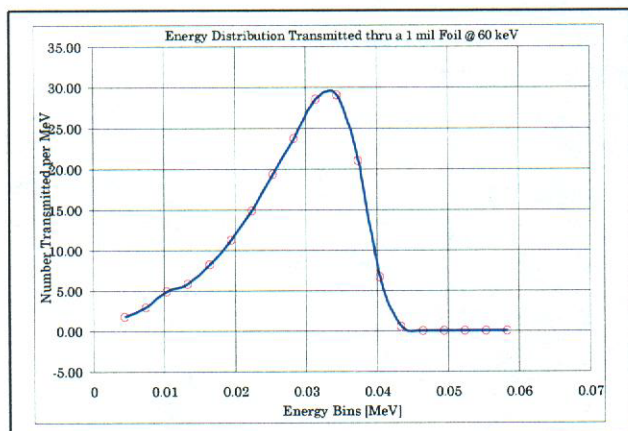


**Figure 7.** Results of a CYLTRAN run showing the energy distribution of the electron beam emerging from the 1 mil Beryllium foil.

Energy deposition in the foil was also determined from the CYLTRAN analysis. Specific heat, density, modulus of elasticity and yield stress were obtained as a function of temperature. Foil heating was then calculated from numerical integration and it was determined that the foil would reach 411°C and 45.5% of yield after a 5 ms pulse. A current density of 15 mA/cm<sup>2</sup> was initially proposed, but this analysis revealed that the foil wouldn't survive the longer pulse. Tensile stresses in the foil were calculated using formulations from Roark [7].

Heating of the stainless steel hibachi was calculated based upon energy depositions from CYLTRAN and the assumption that heating was adiabatic. This yielded a surface temperature of more than 4300°C at the end of the pulse, Fig. 8, which would result in ablation. This high temperature is due to the fact that all of the energy is deposited within 0.001 cm of the surface. In 5 ms, however, the energy diffuses out of this layer, so when thermal diffusion was included in the calculation it was found that the hibachi temperature would only rise to about 242°C.

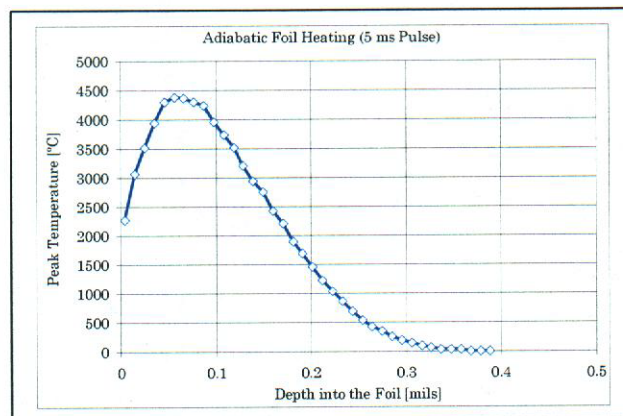


**Figure 8.** The energy distribution in the surface of the stainless steel hibachi, from CYLTRAN.

## V. CONCLUSIONS

A brief overview of the design of a novel multi-cathode electron gun has been given. Some of the tools key to the design were discussed. Issues that complicated the design including the presence of a strong magnetic field, limited space at the output of the gun, cross talk between the independently pulsed cathodes and low energy of the beam were presented. The use of the design tools to solve these problems and the resultant solutions were discussed. Focus was on the most interesting problems and solutions and many issues and detailed calculations had to be omitted for brevity.

## VI. REFERENCES

1. TriComp for Windows, Field Precision, PO Box 13595, Albuquerque, NM, (505) 296-6689, <http://www.fieldp.com>,
2. J. A. Halbleib, R. P. Kensek, T. A. Mehlhorn, G. D. Valdez, S. M. Seltzer and M. J Berger, "ITS Version 3.0: The integrated TIGER Series of Coupled Electron/Photon Monte Carlo Transport Codes," Sand Report: SAND91-1634, UC-405, March 1992.
3. The Handbook of Microwave Technology, Vol. 1 (1995). Particularly note the reference made to Armand Staprans at Varian cited on pg. 538.
4. Rod Latham, "High Voltage Vacuum Insulation," Academic Press, 1995, pp. 119-128, ISBN 0-12-437175-2.
5. J. W. Gewartowsky and H. A. Watson, "Principles of Electron Tubes," D. Van Nostrand Co., Inc., 1965, p. 42.
6. Willis W. Harman, "Fundamentals of Electronic Motion," McGraw-Hill Book Company, Inc., 1953, pp. 136-139, Library of Congress Catalog Card Number: 52-13456.
7. Warren C. Young, "Roark's Formulas for Stress & Strain," Sixth Edition, McGraw-Hill, Inc., 1989, pp. 477-478, ISBN 0-07-072541-1.